New Physics: Sae Mulli,
Vol. 72, No. 6, June 2022, pp. 436∼442
http://dx.doi.org/10.3938/NPSM.72.436

Characterization of a 20-inch Micro Channel Plate Photomultiplier Tube

Geonwoo KIM · Jik LEE · Hongjoo KIM*
Department of Physics, Kyungpook National University, Daegu 41566, Korea

(Received 3 January 2022 : revised 23 February 2022 : accepted 18 April 2022)

There is a proposal to construct a large neutrino detector in Korea, called Korean Neutrino Observatory (KNO), which consists of a large water tank and several tens of thousands of photosensors placed deep underground for neutrino detection. A 20-inch-diameter photosensor including a microchannel plate-photomultiplier Tube (MCP-PMT) is a candidate for the KNO due to its large photo-coverage. We characterized a 20-inch MCP-PMT by measuring its properties, including single photoelectron charge resolution, gain, signal-to-noise performance, dark count rate, after-pulse ratio, and timing performance. We present our measurements of its properties and compare them with those of a previous study.

Keywords: Neutrino, Korean neutrino observatory, Microchannel plate-photomultiplier tube, Photomultiplier tube, Gain, Dark count rate, After-pulse ratio

I. INTRODUCTION

Vacuum-tube-type photosensors are experimental instruments characterized by low noise and high amplification rates that can detect weak light by photoelectric effect and are widely used in astronomy, medicine, biology, chemistry, and physics experiments [1]. The main components of vacuum-tube-type photosensors are photocathode, multiplication part, and anode. The photocathode converts incident photons to photoelectrons. The photoelectrons are accelerated to the multiplication part, where they are multiplied into millions of secondary electrons. Finally, the anode detects the current signal of these electrons. Conventional photomultiplier tube (PMT), microchannel plate-PMT (MCP-PMT), and hybrid Photodetectors (HPDs) are popular vacuum-tube-type photosensors. PMTs have multiple dynodes for multiplication (Fig. 1), whereas MCP-PMTs have microchannel plates for multiplication (Fig. 2). HPDs use avalanche photodiodes as a multiplication device [2]. Large size photosensors are used for large-scale neutrino experiments such as JUNO [3], Super-Kamiokande, Hyper-Kamiokande [4], DUNE [5] experiments. The reason for its large size and spherical shape is to detect the light caused by neutrinos interacting with liquid detectors by being located on the wall of a large-scale liquid tank deep underground. The Korean neutrino observatory (KNO) [6] is a large-scale experiment proposed in Korea to observe neutrinos using the water-Cherenkov phenomenon, which will necessitate characterising and selecting PMTs for the experiment. Among the necessary PMT requirements for KNO's model like Hyper-Kamiocande, the charge resolution is around 50%, the gain is usually 10^7 – 10^8, and the after-pulse ratio is up to 5%. The dark count rate of HQE B&L PMT, a candidate for the Hyper-Kamiocande internal detector, was 8.3 kHz (10^7 gain, at 13 °C) [4].

We investigated the characteristics of a 20-inch MCP-PMT (Fig. 3) delivered from North Night Vision Co., Ltd, China to evaluate the potential use of MCP-PMTs in large-scale neutrino experiments including KNO.

II. EXPERIMENTAL SETUP

In a constant temperature and humidity chamber, the PMT was covered with a shield to prevent light leaks,

*E-mail: hongjoo@knu.ac.kr

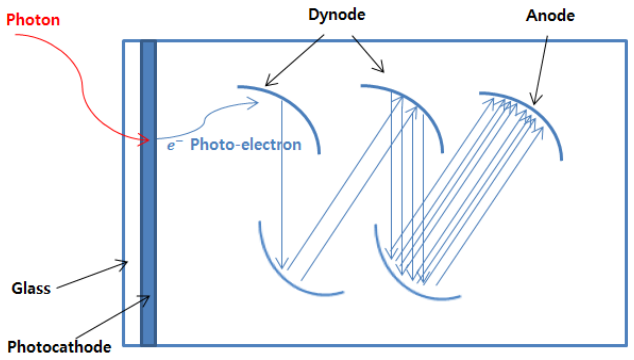

Fig. 1. (Color online) Typical vacuum dynode photomultiplier tube structure: The red line depicts how light strikes the PMT, the blue arrow shows electron direction, and the number of arrows indicates how electrons are amplified at a constant rate as they move through the dynode.

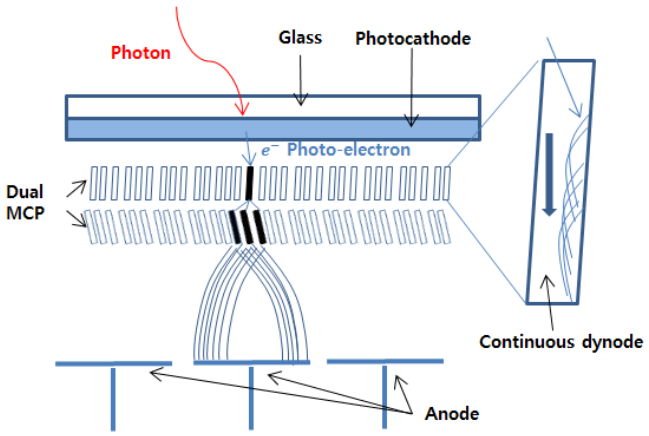

Fig. 2. (Color online) Typical vacuume microchannel plate (MCP)-PMT structure: The red line shows how light is incident on the PMT. The blue arrows and lines are electrons and the number of electrons is continuously amplified in the dynode hole of the MCP. Electrons are directed toward the anode.

and two types of analog-to-digital converters, a function generator, voltage supply, digital oscilloscope, a pre-amplifier, and a data acquisition (DAQ) system were placed next to the chamber. The 780 single photoelectron (SPE) waveforms were obtained using a digital oscilloscope (Waverunner 610zi LeCroy [7]) at room temperature without amplification to measure the rising and falling times. The waveform window was rejected if a 30-mV or higher peak appeared among the triggered signals. The gain and signal-to-noise ratio were measured using a weak light-emitting diode (LED) (light with a wavelength of 505 nm), a flash analogue-to-digital converter (FADC400 Notice Korea [8]) with a 400-MHz sampling rate (Fig. 4). The LED is connected to the function generator via a connector cable, and the light from the LED is transmitted to the PMT via an optical fiber. The LED is generated by a function generator, and the intensity and frequency were set to the number of signals corresponding to SPE, as verified by an oscilloscope. The charge resolution and peak-to-valley ratio were measured with a weak LED light, another analog-to-digital converter (NGT400 Notice Korea [8]) that can measure high rates of signals via waveform analysis and provide the measuring time while calculating the number of waveforms, and 10 times amplification with a pre-amplifier. The after-pulses were measured with a strong LED light (372-nm wavelength and an intensity that can produce a charge of about 229 photoelectrons signals) and FADC400. No light source is used to measure the dark count rate as a function of temperature; rather, a pre-amplifier with a 10-fold amplification is used, and a thermocouple is attached to monitor the temperature while receiving data with the NGT400. The dark count rate is measured using a 1-mV threshold, the after-pulse

Fig. 3. (Color online) 20-inch MCP-PMT : The photocathode of orange color is the transmission photocathode, which is coated on the inner surface of the glass. The reflection photocathode is the silver-coated inside of the glass. MCP is the circular structure in the PMT center. The experimental structure was attached on the top of the PMT.

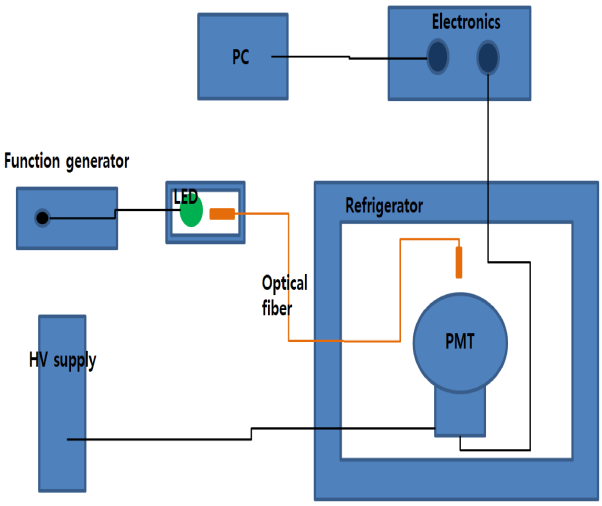

Fig. 4. (Color online) The PMT is installed inside the refrigerator in this figure. The voltage is supplied by an external power source (HV supply) and the PMT signal is converted into a digital signal through electronics and stored in the DAQ system, whereas the LED source is used when necessary.

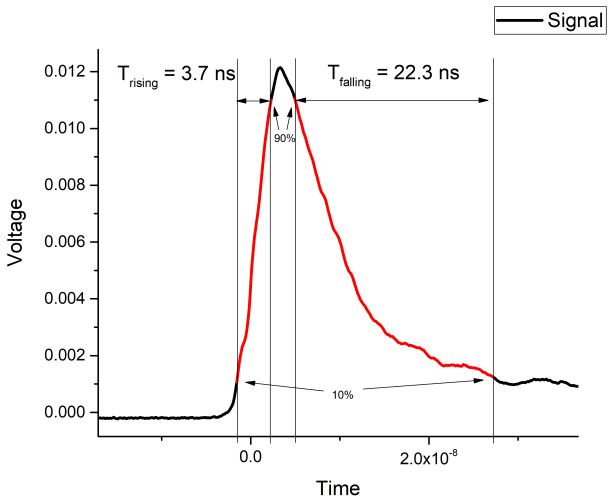

Fig. 5. (Color online) This graph is a signal graph obtained by triggering 780 PMT signals at the same location and averaging them, and the parts corresponding to the rising and falling times are marked in red. The X-axis is time (sec) and the Y-axis is voltage (V).

with a 300-mV threshold, and the rest with a 3-mV threshold that roughly corresponds to 0.25 SPE. In the case of after-pulse counting, pulses with less than 3-mV height were not counted. The operating voltage for all experiments is positive 1,800 volts, which is supplied via a voltage supply device.

III. RESULTS

1. Rising and falling time

In the waveform of a SPE, rising time is the time it takes for a wave to climb from 10% of the peak to 90%, and falling time is the time it takes to decrease from 90% of the peak to 10% (Fig. 5). The timing of signal's up and down is determined by the differences between the PMT positions, where photoelectrons are formed when light strikes the PMT glass and distributions, and the intensities of the MCP electric field [9]. Figure 5 shows that the rising time is 3.7 ns and the falling time is 22.3 ns. The falling time is more than six times the rising time. On average, falling time is two to three times longer the rising time, but the falling time is larger in the 20-inch MCP-PMT. This is because the size, form, and structure of these PMTs differ from those of conventional PMTs, which can be interpreted as a difference caused by the generation location of photoelectrons, among others.

2. Gain

When an electron is created as a photoelectron by the photoelectric effect at the photocathode and travels to anode, the gain is the amplification in terms of the increased number of electrons. This is a significant factor for determining the sizes of charge values in experimental data (Fig. 1 and 2).

The data are obtained using a 3-mV threshold, which is 0.25 times the size of the SPE to FADC400 at room temperature. Figure 6 shows the measured charge distribution of the SPE. Figure 6 shows that the peak of the SPE is at the point where the average value becomes 42.85 ADC. The ADC is the digital value of corresponding analog input without dimensions, and its front is a pedestal area acquired by the intrinsic noise of PMT and electronics. The pedestal region is fitted with an exponential function, and the SPE region is fitted with a Gaussian function. The following formula is used to express the gain [10].

$$G = \frac{(< \mathrm{SPE} > - < \mathrm{PED} >) \times I \times T}{A_{\mathrm{gain}} \times e}$$

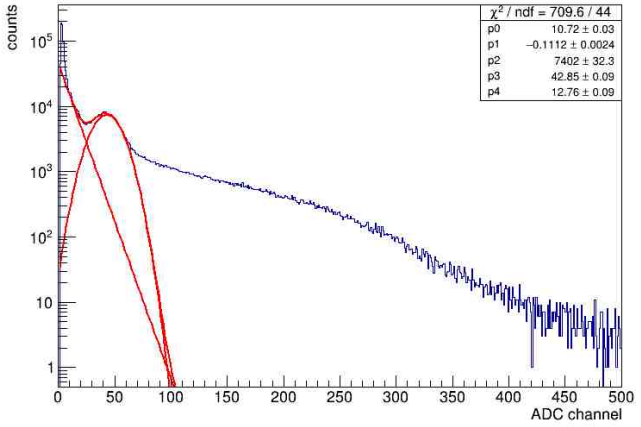

Fig. 6. (Color online) Single photo-electron (SPE) charge distribution with a faint LED source and FADC400 were fitted. The blue line is the distribution graph and the red is the fitting line. The Gaussian-shaped-fitted peak a SPE region, and the region in front of the SPE where the ADC channel is low and the count is high has an exponential shape is a small noise region. The high ADC region to the right of the SPE region is a region of multi photo-electrons and other large noises.

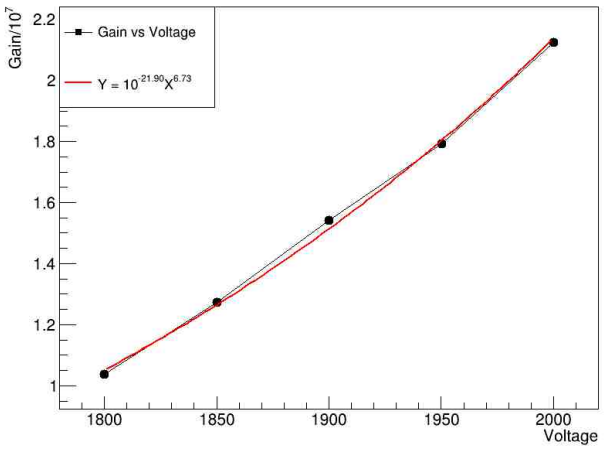

Fig. 7. (Color online) The black line is a graph of gain versus voltage, and the red line is a graph fitted with a multiplier of voltage. The X- and Y-axis represent voltage (V) and gain/10^7, respectively.

The ⟨SPE⟩ is the ADC value of the peak obtained by Gaussian fitting of the SPE, and the ⟨PED⟩ is the ADC value at the peak of the PED(pedestal). (⟨SPE⟩–⟨PED⟩) is set to 42.85. I is the value of volts for one ADC channel, which is $\frac{1}{1024}$ volts divided by 50 Ω of ADC resistance. T represents the sampling time of the ADC channel and is 2.5 ns. A_{gain} is a value related to how much amplification is applied and here it is 1.2. e is the electric charge 1.6×10^{-19} C. North Night Vision Technology (NNVT) provided the gain of this PMT at 9.92×10^6 at DC of 1,802 volts. The gain in Fig. 6 is 1.09×10^7, which is slightly larger than the gain provided by NNVT. Figure 7 depicts a gain vs. voltage graph, which is fitted using a fitting function in the form of a power of voltage. In a typical PMT, dynodes are stacked in stages and electrons arrive at each dynode at a specific rate, which is amplified by the dynodes [9]. Thus, the number of dynodes becomes the exponent of the voltage. The voltage and gain graph are fitted as a function of $Y = a \times X^b$, with variable b equal to 6.73. This metric predicts amplification efficiency compared with a stepwise dynode since the MCP-PMT has a continuous dynode structure.

3. Charge resolution, peak-to-valley ratio, and signal-to-noise Ratio

Magnitude deviations of PMT signal waveforms corresponding to a SPE determine the PMT's charge resolution. The height of a SPE is roughly 11-mV when the gain reaches about 10^7 at an operating voltage of 1,800 volts. The greater the deviation in the height and width of this SPE, the greater the charge resolution of the SPE distribution histogram. A peak-to-valley ratio is the ratio of a SPE's maximum count value to a valley count value between the pedestal and SPE regions of the ADC histogram. A signal-to-noise ratio is the ADC value of a SPE's height divided by the pedestal height's standard deviation. The peak-to-valley ratio and signal-to-noise ratio are determined based on the amplitude and rate of noise. The higher values of these two ratios corresponds to a more uniform signal from the PMT, and a less noise contribution from the PMT, and less interruption from the surrounding environment and electronic devices. The peak-to-valley ratio is a value that is relatively compared between PMTs in the same condition, and the signal-to-noise ratio is the signal amplitude divided by the noise amplitude. If the signal to noise ratio is 3 and the signal height is 3 volts, there is about 1 volt vibration above 3 volts [9]. Figure 8 shows a SPE charge distribution histogram with the NGT400. In the histogram, the pedestal region is fitted with an exponential function, and the

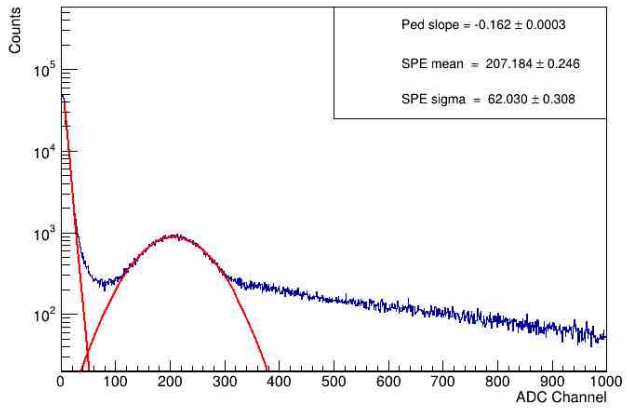

Fig. 8. (Color online) SPE Charge Distribution with faint LED source and pre-amplifier. The distribution graph is represented by the blue line, whereas the fitting line is represented by the red line. The SPE zone is a Gaussian-shaped-fitted peak, and the region in front of the SPE, in which the ADC channel is low and the count is high, has an exponential shape and is a small noise region. Multiphotoelectrons and other large noises can be seen in the high ADC region to the right of the SPE zone.

SPE region is fitted separately with a Gaussian function. The charge resolution is 29.94%, which is calculated by dividing a SPE's standard deviation by its average value and multiplying by 100. The peak-to-valley ratio is 4.98. The signal-to-noise ratio is 6.01.

4. After Pulse Ratio

Signals from a PMT should ideally be caused by the photoelectric effect of the photocathode or the photocathode's thermoelectric emission. However, during the processes of being amplified after being generated and becoming a signal at the anode, a minor spurious signal waveform can be noticed before and after the principal waveform. Small waveforms that follow a specific fixed time are referred to as after-pulses, among these typically unknown waveforms. After-pulses can be divided into two categories. One is the backscattered electrons generated by the amplification structure inside the PMT in a short time after the main pulse. The other type of after-pulses is caused by the remaining amount of gases inside (not fully vacuum). When electrons are generated from the photocathode and accelerated toward amplifying components, they collide with existing gases inside the PMT to produce positive ions.

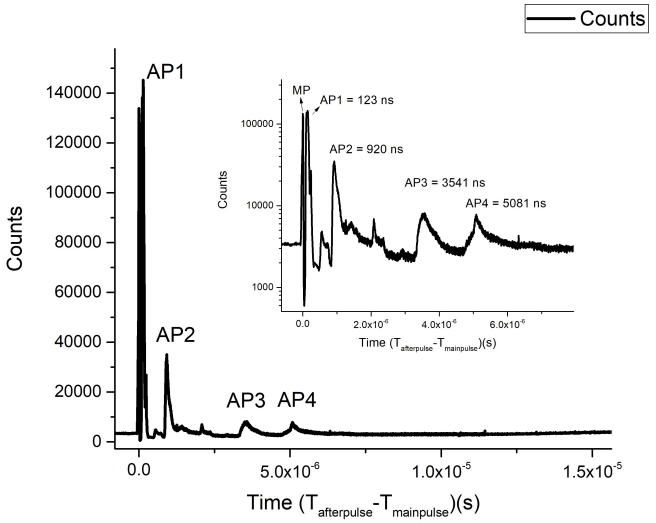

Fig. 9. Time distribution of pulses: MP means main pulse and AP1 – AP4 means after-pulses. The X-axis is the time (s) based on the main pulse, and the Y-axis is the number of pulses. The Y-axis of the inset figure is plotted in log-scale, and the timings is indicated.

Table 1. Pulses Counts and Timing.

Pulse	Counts	Timing (ns)
Main	220000	-
1st AP	1000000	123
2nd AP	390000	920
3rd AP	200000	3541
4th AP	100000	5081

These cations return to the photocathode and generate more photoelectrons, and the pulses caused by these photoelectrons are the second kind of after-pulses. The time range of these second after-pulses is from several hundreds of ns to several tens of μs, depending on the type of existing gases, the generated position, and the applied voltage [9].

The after-pulse ratio can be divided into two categories. One is the ratio produced by dividing the main pulse charge by the charge of the after-pulses. The other is the number of main pulses divided by the number of after-pulses and the number of photoelectron charges of the main pulse [11]. In this study, the method of counting the after-pulse ratio (APR_N) with the number of pulses is obtained as follows:

$$APR_N = \frac{N_{AP}}{N_{MP} \times Q_{MP}} \times 100\%$$

where N_{AP} (the number of after-pulses) is 1690000, N_{MP} (the number of main pulses) is 220000, and Q_{MP} (the

number of photoelectron charges of the main pulse) is 229. The after-pulse ratio was calculated to be 3.35%. Excluding the first after-pulse, which is backscattered electrons, the percentage became 1.37%. Further, the after pulse timing values are consistent with the previous reports [11].

5. Dark Count Rate

The dark count rate is the frequency of a signal corresponding to a SPE emitted from a PMT in a state where the incident light is completely blocked. The thermionic emission from the photocathode and electrode is the main cause of the dark count rate, including current leakage from the PMT electrode and flash emission by cosmic rays as other minor reasons [9]. Thermoelectrons are released even at normal temperature because the photocathode and dynode surfaces are made of low work function materials. The thermoelectric emission law of Richardson can be written as $I = AT^2 \times e^{\frac{-ew}{kT}}$ [9, 12] where I, T, e, w, and A are current, absolute temperature, electron charge, work function, and a constant, respectively, and k is the Boltzmann constant. This formula implies that the lower the temperature, the lower the dark count rate. The SPE area was obtained by subtracting the pedestal area from the histogram after obtaining a SPE charge distribution histogram through the NGT400 and pre-amplifier. To calculate the dark count rate (R_{DC}), the total number of signals (N_{Signal}) are multiplied by the ratio of the SPE entries ($\frac{E_{\mathrm{SPE}}}{E_{\mathrm{Total}}}$) in this histogram, and then divided by total time (T), as shown in the following relationship:

$$R_{\mathrm{DC}} = \frac{E_{\mathrm{SPE}}}{E_{\mathrm{Total}}} \times N_{\mathrm{Signal}}/T$$

In the case of Fig. 10, the number of signals, as calculated by NGT400, is 5.42×10^7 and the total time is 71 s, which results in a calculated dark count of 12.31 kHz. The dark count rate is significant when evaluating signals from a PMT. The large values make it difficult to discern between a physical occurrence and the PMT noise when examining a physical phenomenon, which impedes data interpretation. Because the dark count rate can be quantified using a value that is substantially influenced by temperature, it is critical to observe the eccentricity

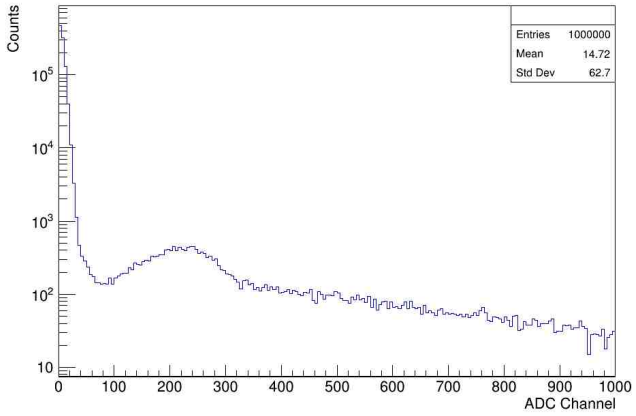

Fig. 10. SPE charge distribution histogram without LED source by NGT400 and pre-amplifier. The total entries in the histogram are 1 million, and the lower ADC channels take most of the entries. A single photoelectron peak is visible near the 240 ADC channel.

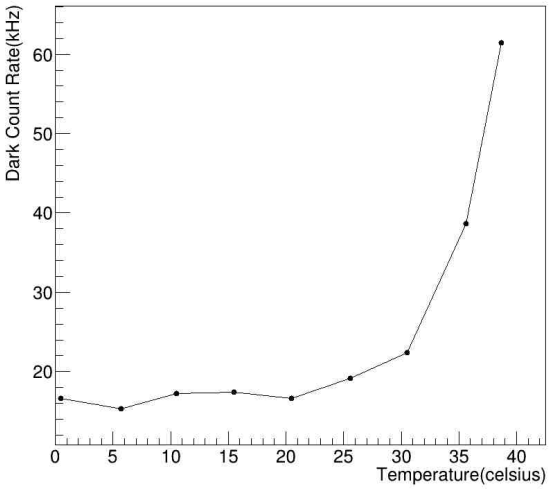

Fig. 11. Dark count rate is plotted as a function of temperature. The fluctuation below 30 °C is small, but increases exponentially above 30 °C.

of the value with respect to temperature, during the experiment. The dark count rate of the PMT is monitored at 5 °C intervals from 0 °C to 40 °C using a constant temperature and humidity chamber, while the temperature is tested by connecting a temperature sensor to the PMT's glass surface. When the temperature dropped below 30 °C, the dark count rate does not change considerably, but it tends to increase exponentially when the temperature is increased beyond 30 °C (Fig. 11). A pattern similar to these results was confirmed in another study [13].

Table 2. Comparison of the data sheet provided by the NNVT company and the results of these experiments (operated at 1800 voltage).

Parameters	NNVT's Data	Results
Gain	9.92×10^6	$(10.89 \pm 0.02) \times 10^6$
charge resolution	28.77%	(29.94 ± 0.18)%
Dark count rate	12.15 kHz	(12.31 ± 0.09) kHz
Peak to valley ratio	9.3	5.0
Rising time	3.62 ns	3.70 ns
Falling time	11.89 ns	22.30 ns
After pulse ratio	0.36%	3.35%

IV. DISCUSSION

Table 2 shows a comparison of the PMT data produced by NNVT Ltd with our obtained experimental results 2. The gain, charge resolution, dark count rate, and rising time are nearly identical to the company-provided reports. However, the peak-to-valley ratio is lower and the falling time is larger than provided specifications. The gain value, which is higher than the manufacturer's report, is within the range of acceptance because the PMTs of the same structure can have a wide range of different gain values. According to the report, the after-pulse counting ratio and the charge ratio of after-pulses for HQE-MCP-PMT [11], the after pulse count ratio is about 1.39%. However, in this study, it is higher than expected.

Because the KNO's experimental structure is similar to that of the Hyper-Kamiokande, it is necessary to satisfy the PMT requirement of the Hyper-Kamiokande. Thus, this PMT's energy resolution, gain, and after-pulse ratio satisfy the requirements [4].

V. CONCLUSION

Investigating the properties of large-size photosensors, including 20-inch MCP-PMTs, and establishing precise characterization methods are crucial for future large-scale neutrino experiments. We have successfully obtained results similar to those reported in other studies. The performance of the MCP-PMT is consistent with previous experimental data, and other characteristics will be investigated soon.

ACKNOWLEDGEMENTS

This work was supported by National Research Foundation grants 2018R1A6A1A06024970 and 2019R1I1A2A02052571 in Korea. The authors wish to thank Sen Qian from the Institute of High Energy Physics of the Chinese Academy of Sciences, Ling Ren from North Night Vision Technology Co., Ltd, China, and the MCP-PMT cooperation group, China for their contribution to insightful discussion on MCP-PMT test.

REFERENCES

[1] R. G. Wagner *et al.*, *The next generation of photo-detectors for particle astrophysics*, arXiv Preprint arXiv:0904.3565 (2009).

[2] Y. Nishimura, International Workshop on New Photon-detectors (LAL Orsay, France, June 13–15, 2012) (https://pos.sissa.it/158/050/pdf).

[3] F. An *et al.*, J. Phys. G: Nucl. Part. Phys. **43**, 030401 (2016).

[4] K. Abe *et al.*, *Hyper-Kamiokande design report*, arXiv Preprint arXiv:1805.04163 (2018).

[5] R. Acciarri *et al.*, *Long-baseline neutrino facility (LBNF) and deep underground neutrino experiment (DUNE) conceptual design report, volume 4 the DUNE detectors at LBNF*, arXiv Preprint arXiv:1601.02984 (2016).

[6] Hyper-Kamiokande proto-Collaboration *et al.*, Prog. Theor. Exp. Phys. **2018**, 063C01 (2018).

[7] Teledyne Lecroy. https://teledynelecroy.com/

[8] Notice Korea. https://www.noticekorea.com/

[9] Hamamatsu Photonics. Photomultiplier Tubes.

[10] S. Aiello *et al.*, J. Instrum. **13**, P05035 (2018).

[11] Q. Wu *et al.*, Nucl. Instrum. Methods Phys. Res. A **1003**, 165351 (2021).

[12] R. L. Bell, *Negative electron affinity devices* (Oxford University Press, USA, 1973).

[13] H. Li *et al.*, J. Instrum. **15**, T08004 (2020).